

## Positron affinity in semiconductors: Theoretical and experimental studies

J. Kuriplach

*Department of Low Temperature Physics, Charles University, V Holešovičkách 2, CZ-180 00 Prague 8, Czech Republic*

M. Šob

*Institute of Physics of Materials, Academy of Sciences of the Czech Republic, Žitkova 22, CZ-616 62 Brno, Czech Republic*

G. Brauer, W. Anwand, and E.-M. Nicht

*Forschungszentrum Rossendorf, Postfach 510119, D-01314 Dresden, Germany*

P. G. Coleman

*School of Physics, University of East Anglia, Norwich NR4 7TJ, United Kingdom*

N. Wagner

*Fachbereich Physik, Martin-Luther-Universität Halle-Wittenberg, Friedemann-Bach-Platz 6, D-06108 Halle/Saale, Germany*

(Received 14 May 1998)

Knowledge of the positron affinity  $A_+$ , a basic bulk characteristic of materials, is important to the understanding of positron trapping at interfaces and at precipitates. Theoretical calculations of  $A_+$  for 3C, 4H, and 6H polytypes of SiC, based on various approaches to electron-positron correlations within the local-density approximation and the generalized gradient approximation for positrons, are compared with experimental values obtained via work-function measurements. The disagreement between theoretical and experimental values of  $A_+$  is discussed in terms of difficulties in the precise measurement of the positron work function and the possible inadequacy of contemporary approaches to electron-positron correlation in semiconductors. [S0163-1829(99)02303-6]

### I. INTRODUCTION

Positrons can serve as a very efficient and sensitive probe of the electronic and atomic structure of condensed matter. Over the last two decades the development of positron spectroscopies of the solid state has become very dynamic, with both theory and experiment contributing to this process. The slow-positron beam technique<sup>1,2</sup> is now a well-established tool for the study of defect depth distributions close to the surface of materials.<sup>2</sup> Re-emitted positron spectroscopy (RPS) can be used to study the re-emission of positrons implanted into a sample.<sup>3</sup> From the energy spectrum of such positrons some fundamental, energy-related properties of the system studied can be derived.<sup>3,4</sup> Recently, we have used RPS to measure the positron work function  $\phi_+$ , and hence an “experimental” value of  $A_+$ , for 6H and 3C polytypes of SiC.<sup>5,6</sup> Using a standard *ab initio* calculational method we determined theoretical values for  $A_+$  for both polytypes,<sup>7</sup> allowing a direct comparison of experimental and theoretical values for a semiconducting system. The disagreement between experiment and theory prompted the present work on 3C-, 4H-, and 6H-SiC.

The electron-positron correlation energy utilized in most contemporary calculations originates from the calculations of Arponen and Pajanne,<sup>8</sup> who theoretically determined characteristics of electron-positron interactions for an ideal case of one positron placed in a homogeneous electron gas (i.e., for a vanishing positron density). Later Lantto<sup>9</sup> performed calculations for a few nonzero ratios of the positron and elec-

tron density. Results of these numerical calculations<sup>8,9</sup> of the electron-positron correlation energy and the electron enhancement factor were parametrized by Boroński and Nieminen,<sup>10</sup> who obtained an analytical formula suitable for use in standard electron structure calculational schemes into which positrons can be incorporated within the framework of the local density approximation<sup>10–12</sup> (LDA). It is usual to assume a vanishing positron density, which simplifies the theory considerably.

The electron enhancement factor and the positron correlation energy based on homogeneous electron-gas results are appropriate for metallic systems only, where positrons are well screened due to the delocalized electrons in the conduction band. For systems with a band gap, where the positron screening is incomplete, some corrections have to be included. Puska *et al.*<sup>13</sup> introduced two different models for semiconducting and insulating materials. In rare-gas solids, the situation is even more complicated, as the LDA breaks down, and an approximation based on polarizability of atoms has to be applied.<sup>14</sup> Recently, an approach to the electron-positron correlations based on the generalized gradient approximation<sup>15</sup> (GGA) has been formulated.<sup>16</sup> We have applied all these models to the 3C, 4H, and 6H polytypes of SiC to test their ability to reproduce both the positron affinity  $A_+$  and the positron lifetime  $\tau$  obtained in experiment.

In Sec. II theoretical principles and methods are described. Section III describes the experimental method, and in Secs. IV and V the results are presented and discussed.

## II. THEORETICAL METHODS AND CONCEPTS

### A. Electronic structure and positron state calculations

To calculate the electronic structure of the systems studied, the linear muffin-tin orbital (LMTO) method<sup>17</sup> within the atomic sphere approximation has been employed. Details of calculations are described elsewhere.<sup>7</sup> Electron exchange-correlation effects are treated in a standard way within the LDA for electrons<sup>18</sup> using the von Barth and Hedin form of the exchange-correlation potential.<sup>19</sup> It is well known that the LDA systematically underestimates the size of band gaps in semiconductors and insulators.<sup>18</sup> For calculations of  $A_+$  the energetics are important (see below), and one has to be careful when experimental and theoretical values are compared.

Positrons may be included into calculations in the following way. Suppose that the positron density is vanishing in the whole system, so that the electronic structure is not influenced by the presence of a positron. Under such conditions we can independently calculate the electronic structure and then solve a Schrödinger-like equation to obtain the positron states and energies (for a thermalized positron it is appropriate to consider that a state with the lowest energy is its ground state). This scheme, used in all our calculations, is called the zero positron density approximation, and is exact for a periodic (bulk) system without positron traps (i.e., in which a positron is delocalized).

Within the approach adopted the positron potential  $V_+$  can be written as a sum of two terms,<sup>11</sup>

$$V_+(\mathbf{r}) = -V_{Coul}(\mathbf{r}) + V_{corr}(\mathbf{r}), \quad (1)$$

where  $V_{Coul}(\mathbf{r})$  is the Coulomb potential for electrons, and  $V_{corr}(\mathbf{r})$  is the correlation potential. Both terms depend on the electron density  $n_-(\mathbf{r})$  and in this sense we are using an LDA theory (except the GGA and rare-gas solid models; see below).

If the material contains some defects, which can act as positron traps, the positron density is not negligible in some parts of the system, and the two-component density functional theory should be used.<sup>10</sup> Surprisingly, the zero positron density approximation works reasonably even for such cases, and we refer to Refs. 10, 11, and 20 for further discussion.

To calculate the positron annihilation rate  $\lambda$  (the inverse of the positron lifetime  $\tau$ ) the well-known formula<sup>11</sup>

$$\lambda = \tau^{-1} = \pi r_e^2 c \int n_-(\mathbf{r}) n_+(\mathbf{r}) \gamma(\mathbf{r}) d\mathbf{r} \quad (2)$$

is used, where  $n_+(\mathbf{r})$  is the positron density,  $\gamma(\mathbf{r})$  is the enhancement factor,  $r_e$  is the classical electron radius, and  $c$  is the speed of light.

### B. Positron affinity

Let us consider a solid consisting of two phases. From the energy point of view, positrons “prefer” one of these phases (as they are not the same), i.e., the “affinity” of positrons to one of these phases is larger. This notion of the positron affinity,  $A_+$ , was introduced in Ref. 21 and further developed in Ref. 22. Sometimes, however,  $A_+$  is understood in terms of “attractivity” to positrons of different atoms inside materials containing more than one atomic component, or, in

other words, preferential positron occupation or annihilation.<sup>23</sup> In what follows we shall use only the first meaning of the  $A_+$  mentioned above.

The positron affinity is defined by the simple relation<sup>22</sup>

$$A_+ = \mu_- + \mu_+, \quad (3)$$

where  $\mu_-$  and  $\mu_+$  are the electron and positron chemical potentials, respectively.  $\mu_+$  may be identified with the lowest positron energy. But  $\mu_-$  is determined from the electron band filling (in the case of semiconductors  $\mu_-$  is taken to be at the position of the top of the valence band). Both  $\mu_-$  and  $\mu_+$  are defined with respect to the same zero energy level (the so called “crystal zero”; see a detailed discussion in Ref. 22).  $A_+$  as defined in Eq. (3) can be related to the electron and positron work functions ( $\phi_-$  and  $\phi_+$ ) by the equation<sup>22</sup>

$$\phi_- + \phi_+ + A_+ = 0. \quad (4)$$

This can be easily proved if we consider relations between respective chemical potentials and work functions  $\phi_{\pm} = -\mu_{\pm} \mp \Delta$ , where  $\Delta$  is the surface dipole barrier (we use the same sign conventions as in Ref. 22).

These two independent definitions of  $A_+$  correspond to the two ways in which this quantity can be obtained. Usually Eq. (3) is used by theoreticians to calculate  $A_+$  as the dipole barrier  $\Delta$  is not accessible within standard calculational electron structure methods. Experimentalists prefer Eq. (4) as electron and positron work functions are measurable quantities. For completeness, we should notice the relation between  $A_+$  and the positronium formation potential,<sup>11,24</sup> which can also be used, in principle, in a measurement of  $A_+$ .

$A_+$  is a bulk material property. Nevertheless, its practical usage concerns material surfaces and interfaces. If two distinct materials ( $A$  and  $B$ ) are in contact, the electron chemical potentials align mutually and, therefore, the difference between the  $A_+$  values is equal to the difference between positron levels in these two materials:<sup>21,22</sup>

$$\Delta A_+^{A,B} = A_+^A - A_+^B. \quad (5)$$

If  $B$  is a precipitate, the relation  $\Delta A_+^{A,B} > 0$  represents a necessary condition for positron trapping in this precipitate.

To our knowledge, all calculations of  $A_+$  to date have been performed using the LMTO method, and for elemental metals the results agree very well with experimental data, as documented in recent reviews.<sup>11,12</sup> On the other hand, there has been no systematic comparison for semiconductors, as experimental values of  $\phi_+$  have not been available for this type of material (except perhaps diamond<sup>25</sup> which is, however, usually treated as an insulator).

### C. Positron correlation potential

Comparison of calculated and experimental values of  $A_+$  for a semiconducting system provides a serious test of electron-positron correlation theory. In this section we shall discuss various theoretical approaches to electron-positron correlations, corresponding correlation potentials, and enhancement factors. Most of the present calculations in metals are done utilizing the results of Arponen and Pajanne<sup>8</sup> for the electron-positron correlation energy, parametrized by Borón-

ski and Nieminen;<sup>10,26</sup> we shall refer to these as BN calculations, and the corresponding correlation potential will be denoted as  $V_{BN}$ . The  $A_+$  values calculated using this potential agree well with experiment, at least for elemental metals.<sup>11,12,22</sup> In the work described in Ref. 10, an interpolation formula for the electron enhancement factor is also given:

$$\gamma_{BN}(r_s) = 1 + 1.23r_s + 0.8295r_s^{3/2} - 1.26r_s^2 + 0.3286r_s^{5/2} + r_s^3/6. \quad (6)$$

Here is  $r_s = \sqrt[3]{3/(4\pi n_-)}$  the electron density parameter. This enhancement, however, is not consistent with  $V_{BN}$ , as  $\gamma_{BN}$  comes from a parametrization of the results of Lanto,<sup>9</sup> who used an approach to electron-positron correlations in a homogeneous electron gas qualitatively different to that of Arponen and Pajanne<sup>8</sup> (see below).

Due to incomplete positron screening in systems with a band gap, the electron-positron correlation energy and the enhancement factor have to be modified. Puska *et al.*<sup>13</sup> introduced two distinct electron enhancement factors which are able to reproduce experimental positron lifetimes for semiconductors and insulators. We shall call the corresponding physical models the ‘‘semiconductor model’’ (SM) and the ‘‘insulator model’’ (IM), as in Ref. 13. The idea of the SM is that a positron in a semiconducting material is screened electrostatically (as in a dielectric material described by the static dielectric constant  $\epsilon$ ). The derivation<sup>13</sup> leads to the modification of the last term in Eq. (6) which is multiplied by the factor  $(1 - 1/\epsilon)$ ; the resulting enhancement will be denoted by  $\gamma_{SM}$ . The enhancement factor within the IM is expressed as a linear function of atomic polarizability, and thus to the dielectric constant through the Clausius-Mossotti formula, i.e.,

$$\gamma_{IM} = 1 + A + B \Omega (\epsilon - 1)/(\epsilon + 2). \quad (7)$$

The values of the two adjustable parameters  $A = 0.684$  and  $B = 0.0240a_0^{-3}$  were found by comparing calculated and measured lifetimes for selected systems;<sup>11-13</sup>  $\Omega$  is the volume per atom and  $a_0$  is the Bohr radius.

The correlation potentials  $V_{SM}$  and  $V_{IM}$  can be easily obtained using the general scaling relation for the positron correlation potential  $V_{corr}$ ,<sup>11,13,27</sup>

$$V_{corr} \propto (\lambda - \lambda_{IPM})^{1/3}, \quad (8)$$

where  $\lambda_{IPM}$  is the annihilation rate within the IPM [i.e., with no enhancement ( $\gamma_{IPM} = 1$ )]. Then if  $\lambda_{SM,IM,BN} = \lambda_{IPM} \gamma_{SM,IM,BN}$ ,

$$V_{SM,IM} = V_{BN} \left( \frac{\gamma_{SM,IM} - 1}{\gamma_{BN} - 1} \right)^{1/3}. \quad (9)$$

For rare-gas solids the following form of the correlation potential was adopted (using atomic units):

$$V_{RGSM}(r) = - \frac{\alpha}{2(r^2 + r_1^2)^2} \quad (10)$$

(RGSM means ‘‘rare-gas solid model’’).  $\alpha$  is the atomic polarizability,  $r$  is the distance from the nucleus and  $r_1$  is a model parameter fixed at value 1.7  $a_0$  to obtain good

agreement with experiment.<sup>14</sup>  $V_{RGSM}$  does not depend on the electron density and its radial dependence stems from the polarization of the atom by positrons,<sup>28</sup> which is an appropriate approach for rare-gas solids. To test the validity of this approximation for the SiC system, we use an average value of the atomic polarizability for Si and C atoms derived from the static dielectric constant, using the Clausius-Mossotti relation.

The application of the GGA to electron-positron correlations<sup>16</sup> leads to a unified treatment of metals and systems with a band gap. The spirit of this approach consists in reducing the LDA enhancement factor  $\gamma_{LDA}$  according to the inhomogeneity of the electron density (measured by its gradient) at the positron site. A new form of  $\gamma_{LDA}$ , consistent with the correlation potential  $V_{BN}$ , has been found to be

$$\gamma_{LDA}(r_s) = 1 + 1.23r_s - 0.0742r_s^2 + r_s^3/6 \quad (11)$$

(cf. Ref. 29). The corresponding enhancement within the GGA is then<sup>16</sup>

$$\gamma_{GGA} = 1 + (\gamma_{LDA} - 1) \exp(-\beta\epsilon). \quad (12)$$

Here  $\beta$ , a model parameter which is adjusted so that the lifetimes calculated within this approach agree well with experiment for several selected systems, is found to have the value 0.22.<sup>16</sup>  $\epsilon$ , proportional to  $|\nabla n_-|^2/n_-^2$ , characterizes the gradient of the electron density  $n_-$ .<sup>16</sup> The resulting electron-positron correlation potential is given by the formula

$$V_{GGA} = V_{BN} \exp(-\beta\epsilon/3), \quad (13)$$

which can be derived using Eq. (9) if  $\gamma_{BN}$  is replaced by  $\gamma_{LDA}$  and  $\gamma_{SM,IM}$  by  $\gamma_{GGA}$ .

### III. EXPERIMENTAL METHODS

To obtain experimental values of  $A_+$  the two quantities  $\phi_-$  and  $\phi_+$  must be measured [see Eq. (4)].

#### A. Properties related to electronic structure

The distance from the top of the valence band to vacuum ( $\phi_-$ ) for all SiC polytypes has been determined using the experimental electron affinity  $\chi_-$  and energy-band gap  $E_g$ , which have been measured via the contact voltage retarding potential method<sup>7,30</sup> and photoacoustic spectroscopy,<sup>31</sup> respectively. Then  $\phi_- = \chi_- + E_g$ .

The experimental setup for contact potential measurements is described in Ref. 30. As shown there, the contact potential appears between the metal (tungsten)-vacuum surface, considered as a reference, and the SiC-vacuum surface; both surfaces being placed in an ultrahigh vacuum at a distance of 1.0 mm from each other. According to that, quasi-macroscopic space-charge effects are important for thermodynamic equilibrium only. In this case the Schottky barrier (related to maximum band bending) has to be overcome when an electron is excited from the metal into the conduction band of SiC. Hence we adopt the Schottky model,<sup>32</sup> and the electron affinity for 4H-SiC can be derived using the simple relation  $\chi_- = eU_{CP} + \phi_w$ , where  $U_{CP}$  is the contact potential and  $\phi_w$  [= 4.50 eV (Ref. 30)] is the electron work function for tungsten. Both quantities are true bulk properties

from which dipole effects (microscopic interface dipoles giving rise to change the band bending and Fermi level pinning) are excluded.

The basic mechanism of the photoacoustic effect is that optical absorption takes place in a sample when illuminated by intensity modulated light. The sample is thus heated intermittently by nonradiative electronic transitions. This periodic heating as photoacoustic response generates inelastic (thermoacoustic effect) and elastic (thermoelastic effect) strains which can be detected by lead-zirconium-titanate (PZT) transducers.

The optical arrangement consists of 300-W xenon lamp, interference filters (a full width at half maximum of 10 nm), a light chopper, and an open photoacoustic cell. This cell has been made of 4H-SiC sample and PZT transducer, both attached opposite to a thin alumina disc with a hard-setting conductive carbon cement. The light transmission through the sample for energies smaller than the indirect 4H-SiC energy gap produces low-frequency stress-strain signals in the Al-support which are proportional to the exciting light intensity (photoacoustic saturation<sup>31</sup>). The signal from the transducer is fed into a charge preamplifier, whose output goes to a narrow bandpass filter and then into a dual phase lock-in amplifier.

In the range of photoacoustic saturation the signal intensity can be regarded as independent of the absorption coefficient. In this case the normalized intensity is constant. However, when the light energy is greater than the fundamental energy gap of the semiconductor deposit, the reflection in the range of energies above the gap gives directly the interband transition energies via dips in the saturation intensity.

### B. Positron work function

Current measurements of the positron work function are based on the following facts: (i) if  $\phi_+$  is negative, positrons entering a sample studied and diffusing back to its surface can escape the sample; and (ii) the maximum kinetic energy of such re-emitted positrons is equal to  $-\phi_+$ . In practice, a variable retarding potential is applied to the sample to obtain the energy spectrum of re-emitted positrons. The positron work function is then determined from an analysis of this spectrum.

Our measurements of the positron work function have been carried out on the magnetic-transport positron beam at Norwich.<sup>33</sup> Count rates of gamma rays resulting from the annihilation of positrons in the sample are measured as a function of sample potential. First, the zero potential  $V_0$  is determined, being the highest sample potential at which no re-emitted positrons are returned to the sample. Second, the potential  $V_B$  is determined, being the lowest energy at which all thermalized and re-emitted positrons are returned to the sample surface. Then  $\phi_+ = V_B - V_0$ .

## IV. RESULTS AND DISCUSSION

### A. Properties related to electron structure

In Fig. 1 the photoacoustic spectrum of the 4H-SiC polytype is presented. The two broad absorption structures at 2.07 and 3.27 eV result from optically excited energy levels

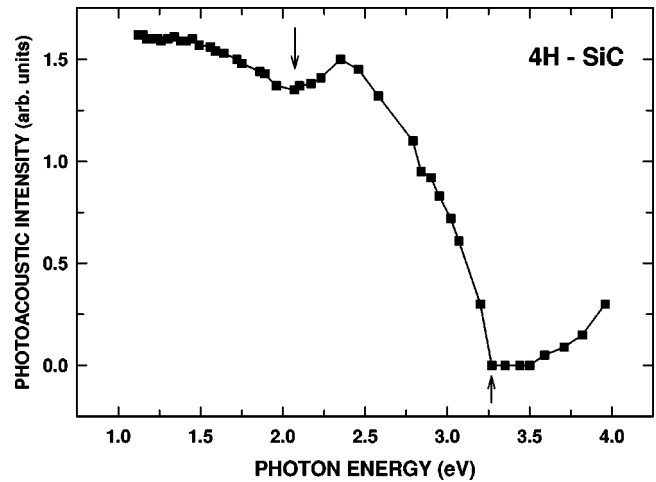


FIG. 1. Photoacoustic spectrum measured for the 4H-SiC sample. Two vertical arrows mark the dips discussed in the text.

which decay into two channels reducing the photoacoustically saturated signal through radiative transitions. Both shallower-sloped structures are a result of indirect interband transitions. The major dip at 3.27 eV corresponds to  $\Gamma_{6v}-K_{2c}$  transition of the 4H-SiC polytype [3.2 eV (Ref. 34)]. The 2.07-eV dip is due to transitions at  $\Gamma_{15v}-X_{1c}$  [100] of 3C-SiC. Because of the shallow slope and energies involved,<sup>35</sup> the influence of active dopants can be excluded. The shift from 2.35 eV (Ref. 6) to lower energy is caused by a surface effect with fewer bonding neighbors. We thus notice a polytype change from hexagonal 4H modification to the cubic 3C-SiC one in a thin layer deposit (approximately 5 nm can be deduced from the intensity attenuation).

This interpretation is further supported by the current-voltage characteristics in the retarding potential measurement for our sample which reaches saturation current at an unexpected bias of  $U_{CP} = -2.62$  eV (see Fig. 2). For the 3C-SiC/4H-SiC semiconductor heterostructure the (more covalent) 3C wave functions leak into the gap of the 4H substrate. Therefore, the measured bias voltage has to be corrected for dipole effects from  $-2.62$  eV to  $[-2.62$  eV +

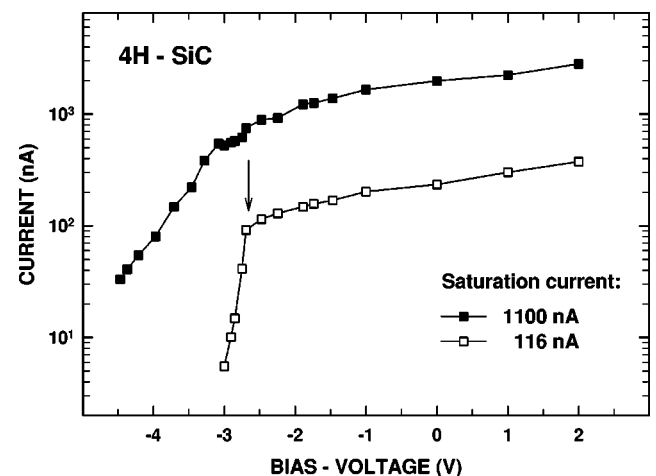


FIG. 2. Residual/saturation current-voltage measurements on a two-electrode tube (cathode: W; anode 4H-SiC) under ultrahigh-vacuum conditions ( $10^{-9}$  Torr). The vertical arrow marks the position of  $U_{CP}$  (see the text).

TABLE I. Experimental values of electron affinities ( $\chi_-$ ), positron work functions ( $\phi_+$ ), electron band gaps ( $E_g$ ; theoretical values are given in brackets), distances from the top of the valence band to the vacuum level ( $\phi_-$ ), and experimental value of positron affinity ( $A_+$ ) for three SiC polytypes. Experimental errors are indicated below the symbols  $\chi_-$ ,  $E_g$ , and  $\phi_-$ , and in parentheses after the tabulated values of  $\phi_+$  and  $A_+$ . All values are in units of eV.

Polytype	$\chi_-$ ( $\pm 0.05$ )	$E_g$ ( $\pm 0.2$ )	$\phi_-$ ( $\pm 0.25$ )	$\phi_+$	$A_+$
3C	3.83	2.35 [1.50]	6.18	-2.35 (0.20)	-3.83 (0.45)
4H	3.08	3.27 [2.57]	6.35	-2.17 (0.25)	-4.18 (0.50)
6H	3.34	3.17 [2.28]	6.51	-2.10 (0.20)	-4.41 (0.45)

$E_g(4H) - E_g(3C) = -1.42$  eV. This correction follows from the Schottky model,<sup>32</sup> aligning the vacuum potential of the two polytypes involved. For this model we assume perfectly matching lattices and no defects at the interface, which is—at least in the former—a tenable assumption for polytypes with the difference of only (Si-C) double layers in their stacking sequences.

The measured values of  $\chi_-$ ,  $E_g$ , and resulting  $\phi_-$ 's for all polytypes studied are presented in Table I (values for 3C and 6H were taken from Refs. 6 and 7, respectively). We note that the differences in  $\phi_-$ 's among polytypes studied lie near the limit of experimental uncertainties.

In Fig. 3 the calculated density of states (DOS) is shown for all three SiC polytypes studied. The DOS curves exhibit clear differences; nevertheless, common features prevail. This reflects the fact that the crystal structure of all SiC polytypes have similarities—namely, that the first coordination sphere of any chosen atom is tetrahedral. The valence band consists of two subbands. The subband located lower in energy is predominantly of *s* character, with both Si and C *s* states contributing. In the second subband C *p* states dominate (Si *s*-like states can also be observed at lower energies). The bottom of the conduction band is mainly of *s* character. Theoretical energy-band gaps can be deduced from the DOS curves presented. Their values are given in Table I (in brackets) together with their experimental counterparts. One can clearly see that theory (LDA) underestimates appreciably this quantity (by about 30%), as we have already mentioned above.

### B. Positron work function

In Fig. 4 the measured integral spectra of re-emitted positron intensities for the three SiC polytypes studied are plotted. We comment here that the observed spectra certainly are dominated by work-function emission from the SiC surface. Three following arguments support this conclusion: (a) the sharpness of the energy spectra at low energies, (b) the persistence of re-emission to relatively high incident positron energies, and (c) the great reduction in re-emitted intensity from defected SiC samples.<sup>5</sup> The extraction of the positron work functions  $\phi_+$  from these spectra is, however, not straightforward, due to epithermal positron emission. This occurs even for incident positron energies as high as 5 keV; the presence of the epithermal component requires evaluation of  $V_B$  by extrapolation. The result for 4H-SiC will be affected by the thin overlayer of 3C polytype (see Sec. IV A), but reference to the bilayer results of Ref. 3 suggests

that the additional experimental uncertainty associated with the presence of this layer is only  $\sim 0.05$  eV.

Results for  $\phi_+$  are listed in Table I. Although the estimated positron work functions do not differ significantly within the limits of present experimental errors, a tendency of increase (of magnitude) is seen when going from 6H to 3C polytype. This conclusion is supported by the fact that at the same time the opposite tendency appears in the experimental values for the electron work function.

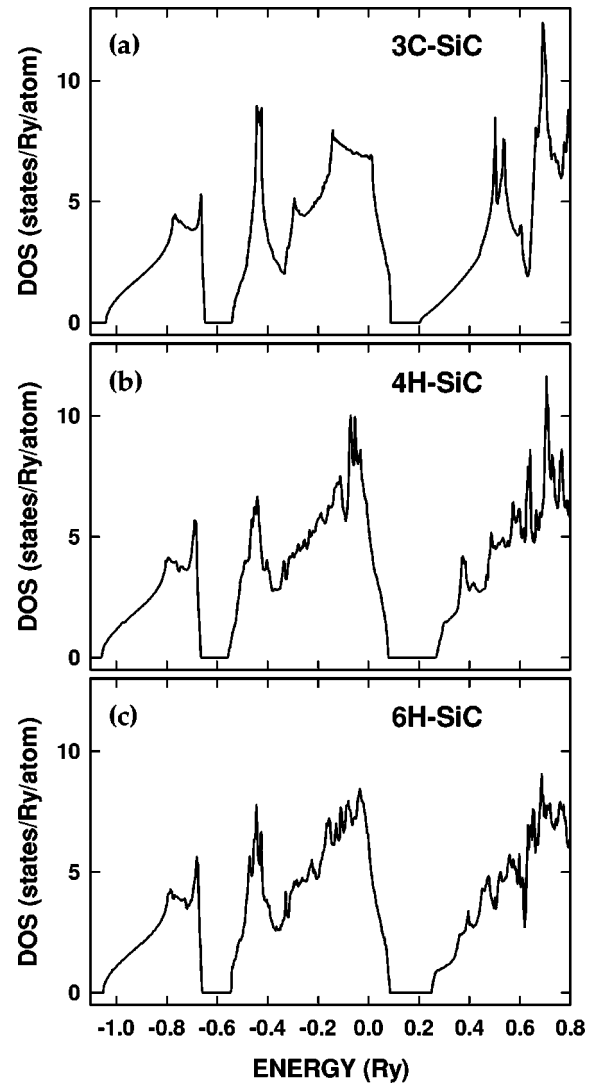


FIG. 3. Density of states for (a) 3C-, (b) 4H-, and (c) 6H-SiC polytypes.

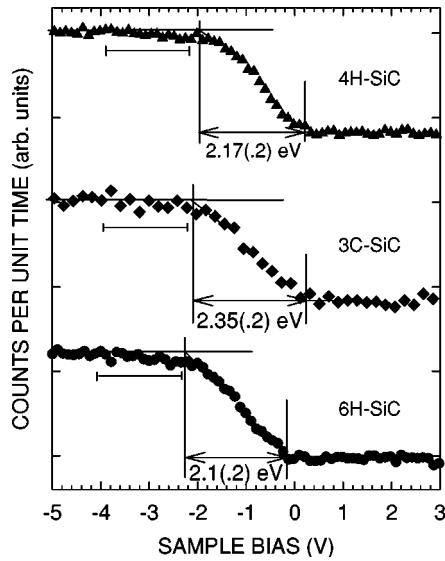


FIG. 4. Integral spectra of re-emitted positrons for 4H, 3C, and 6H polytypes. The horizontal bars on the left indicate the extent of the epithermal positron distributions.

C. Positron affinity

The measured values of  $\phi_-$  and  $\phi_+$  are substituted into Eq. (4) to obtain the values for  $A_+$  shown in Table I. Differences between the three values are rather small, as expected. The values of  $A_+$  calculated using five different forms of electron-positron correlation potential discussed in Sec. II C are shown in Table II. The comparison of experimental and theoretical values of  $A_+$  is visualized in Fig. 5.

An important feature of the theoretical values of  $A_+$  is that there are only very small differences among polytypes investigated. Thus positrons do not seem to be sensitive to details of the crystal structure of SiC polytypes. Likewise, the dependence of the calculated  $A_+$  on the form chosen to describe the electron-positron correlations is generally slight, indicating that the scaling of the positron correlation potential  $V_{BN}$  [see Eqs. (9) and (13)] has only a small influence.

We see that there is an obvious discrepancy between theory and experiment. The best agreement occurs in the case of the insulator model; from the theoretical point of view this is quite unsatisfactory, as the IM is based on a phenomenological approach to the electron-positron correlations and does not provide any explanation of the particular values of  $A$  and  $B$  parameters entering the model (see Sec. II C). One could probably find values of  $A$  and  $B$  which lead to a better accordance with experiment, but the underlying physics remains hidden. In this respect we should note one important point. Three of the five models studied (IM, GGA, and RGSM) contain adjustable parameters which have been

TABLE II. Calculated values of positron affinity ( $A_+$ ) for three SiC polytypes. Various theoretical approaches to electron-positron correlations are used (see the text). All values are in units of eV.

Polytype	BN	SM	IM	GGA	RGSM
3C	-6.07	-5.88	-4.84	-5.61	-8.60
4H	-5.95	-5.76	-4.73	-5.49	-8.51
6H	-5.98	-5.79	-4.76	-5.52	-8.54

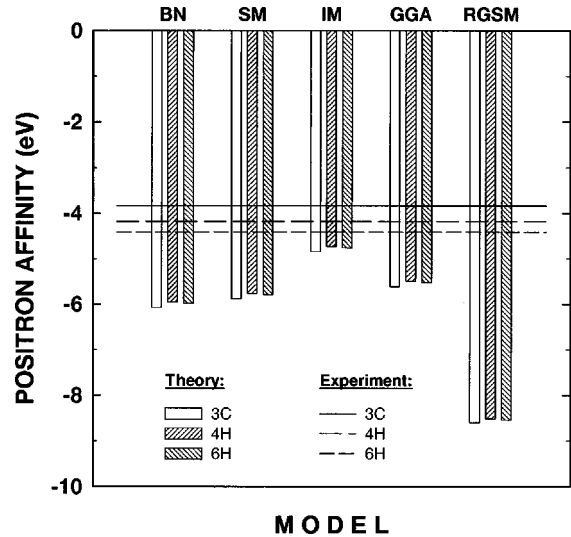


FIG. 5. Comparison of experimental and theoretical values of the positron affinity for all SiC polytypes studied.

found by fitting to experimental positron lifetimes for selected systems (with the exception of the RGSM, where energy properties are fitted). This means that these models are often tuned up to yield “good” lifetimes, not considering other positron-related properties.

In Table III we list calculated positron lifetimes in 6H-SiC for all theoretical models examined (except the RGSM, where it is not possible to calculate the lifetime). We can see that the GGA gives very good agreement with the experimental value<sup>36</sup> (also given in Table III). In the case of the IM the agreement is worse, and the other two models (BN and SM) correspond fairly well to experiment. For example, the GGA approach gives a bulk positron lifetime of 139 ps, with the parameter  $\beta$  set to 0.22. The corresponding value of  $A_+$  is -5.52 eV (see Table II). Increasing the  $\beta$  to 1.00 leads to an unsatisfactorily high positron lifetime of 189 ps, but the value of  $A_+$  changes to -4.15 eV, in much better agreement with the experimental value. We can state, therefore, that we need at least a better phenomenological description of the electron-positron interaction in which both lifetime and  $A_+$  can be fitted. However, a model describing the physics of the problem would be even more desirable.

A closer inspection leads to the conclusion that there are two sources of the observed disagreement between theory and experiment. First, it is a well-known deficiency of the LDA for semiconductors that the position of the electron Fermi level may be incorrectly positioned. The error can be approximated by the deviation of the calculated and measured band gaps, which is about 0.8 eV. This is just a rough estimate, however, as beyond LDA electronic structure technique may shift the position of the valence band in both directions, but we believe the above number is a good mea-

TABLE III. Comparison of experimental and theoretical values of the positron lifetime ( $\tau$ ) for the 6H-SiC polytype. In the case of the RGSM, no enhancement is available to calculate the lifetime.

	expt. (Ref. 36)	BN	SM	IM	GGA
$\tau$ (ps)	140	136	142	157	139

sure of the energy error introduced by the LDA (for the energy region of interest). Second, even if this error is considered, the electron-positron correlation energy in SiC polytypes studied is probably lower (in magnitude) than is supposed in current theoretical approaches (except perhaps rather phenomenological insulator model).

It has yet to be confirmed that this effect is a common feature for semiconducting and insulating materials where positrons are not completely screened. Nevertheless, a revision of present approximations to electron-positron interactions in systems with a band gap seems to be necessary. Recently, a quantum Monte Carlo technique has been applied to electron-positron correlations in both homogeneous and simple nonhomogeneous systems.<sup>37,38</sup> It might be possible to apply such a technique to real systems (including semiconductors), notwithstanding very large computational demands.

## V. CONCLUSIONS

We have discussed theoretical and experimental aspects of the positron affinity in semiconducting materials, and have presented results of theoretical and experimental studies of this quantity in three polytypes of SiC. To our knowledge, SiC is the first semiconductor where a direct comparison of the experimental positron affinity with its theoretical counterpart has been done. The experimental positron affinity for SiC has been determined owing to a negative positron work function which can be measured using re-emitted positron spectroscopy. In this respect we should mention that, recently, appreciable positron re-emission has been observed for GaN, probably indicating a negative positron work function for this material as well.<sup>39</sup>

The positron affinity of SiC has been obtained experimentally via the electron and positron work functions. When

measuring the electron work function, both photoacoustic and contact potential experiments must be carefully interpreted, as we have observed a thin 3C-SiC layer on the surface of our 4H-SiC specimen. On the other hand, positron work-function measurements for SiC require careful treatment of the contribution of epithermal positrons to the spectrum of re-emitted positrons.

In general, there are rather small differences in values of the positron affinities among SiC polytypes studied both for experiment and theory. However, all approaches to the electron-positron correlations we have used in calculations yield values of the positron affinity which lie below the experimental value. We have debated the possible origins of this discrepancy, concluding that both electron- and positron-related parts of the problem exist. That is, the electron Fermi level might be misplaced due to the inadequate description of semiconductors within the LDA. In order to clarify this point we intend to perform self-consistent, self-interaction-corrected electronic structure calculations<sup>18,40</sup> for SiC. Our estimates of a possible error of the electron Fermi level, however, show that possible shortcomings in the LDA approach cannot be fully responsible for the apparent disagreement between theoretical and experimental values of the positron affinity for all SiC polytypes studied. Electron-positron correlations thus need further investigation; quantum Monte Carlo techniques could represent a possible way toward achieving this goal.

## ACKNOWLEDGMENTS

We are indebted to O. K. Andersen and O. Jepsen for providing their LMTO-ASA code. We thank M. J. Puska and T. Korhonen for permitting the use of their LMTO positron code and for stimulating discussions.

- 
- <sup>1</sup>W. Triftshäuser and G. Kögel, *Phys. Rev. Lett.* **48**, 1741 (1982).  
<sup>2</sup>*Positron Spectroscopy of Solids*, edited by A. Dupasquier and A. P. Mills, Jr. (IOS, Amsterdam, 1995).  
<sup>3</sup>See, e.g., D. W. Gidley and W. E. Frieze, *Phys. Rev. Lett.* **60**, 1193 (1988).  
<sup>4</sup>M. Jibaly, A. Weiss, A. R. Koymen, D. Mehl, L. Stiborek, and C. Lei, *Phys. Rev. B* **44**, 12 166 (1991).  
<sup>5</sup>J. Störmer, A. Goodyear, W. Anwand, G. Brauer, P. G. Coleman, and W. Triftshäuser, *J. Phys.: Condens. Matter* **8**, 89 (1996).  
<sup>6</sup>G. Brauer, W. Anwand, E.-M. Nicht, P. G. Coleman, N. Wagner, H. Wirth, and W. Skorupa, *Appl. Surf. Sci.* **116**, 19 (1997).  
<sup>7</sup>G. Brauer, W. Anwand, E.-M. Nicht, J. Kuriplach, M. Šob, N. Wagner, P. G. Coleman, M. J. Puska, and T. Korhonen, *Phys. Rev. B* **54**, 2512 (1996).  
<sup>8</sup>J. Aronen and E. Pajanne, *Ann. Phys. (N.Y.)* **121**, 343 (1979).  
<sup>9</sup>L. J. Lantto, *Phys. Rev. B* **36**, 5160 (1987).  
<sup>10</sup>E. Boroński and R. M. Nieminen, *Phys. Rev. B* **34**, 3820 (1986).  
<sup>11</sup>M. J. Puska and R. M. Nieminen, *Rev. Mod. Phys.* **66**, 841 (1994).  
<sup>12</sup>R. M. Nieminen, in *Positron Spectroscopy of Solids*, (Ref. 2), p. 443.  
<sup>13</sup>M. J. Puska, S. Mäkinen, M. Manninen, and R. M. Nieminen, *Phys. Rev. B* **39**, 7666 (1989).  
<sup>14</sup>M. J. Puska and R. M. Nieminen, *Phys. Rev. B* **46**, 1278 (1992).  
<sup>15</sup>J. Perdew, *Physica B* **172**, 1 (1991).  
<sup>16</sup>B. Barbiellini, M. J. Puska, T. Torsti, and R. M. Nieminen, *Phys. Rev. B* **51**, 7341 (1995); B. Barbiellini, M. J. Puska, T. Korhonen, A. Harju, T. Torsti, and R. M. Nieminen, *ibid.* **53**, 16 201 (1996).  
<sup>17</sup>For a recent review, see O. K. Andersen, O. Jepsen, and M. Šob, in *Electronic Band Structure and Its Applications*, edited by M. Yussouff (Springer-Verlag, Heidelberg, 1987), p. 1.  
<sup>18</sup>R. O. Jones and O. Gunnarson, *Rev. Mod. Phys.* **61**, 689 (1989).  
<sup>19</sup>U. von Barth and L. Hedin, *J. Phys. C* **5**, 1629 (1972).  
<sup>20</sup>M. J. Puska, A. P. Seitsonen, and R. M. Nieminen, *Phys. Rev. B* **52**, 10 947 (1995).  
<sup>21</sup>O. V. Boev, M. J. Puska, and R. M. Nieminen, *Phys. Rev. B* **36**, 7786 (1987).  
<sup>22</sup>M. J. Puska, P. Lanki, and R. M. Nieminen, *J. Phys.: Condens. Matter* **1**, 6081 (1989).  
<sup>23</sup>See, e.g., Z. Szotek, B. L. Gyorffy, G. M. Stocks, and W. M. Temmerman, *J. Phys. F* **14**, 2571 (1984); J. Kuriplach, M. Šob, and C. Dauwe, *Nukleonika* **42**, 153 (1997).  
<sup>24</sup>P. J. Schultz and K. G. Lynn, *Rev. Mod. Phys.* **60**, 701 (1988).  
<sup>25</sup>G. R. Brandes, A. P. Mills, Jr., and D. M. Zuckerman, *Mater. Sci. Forum* **105-110**, 1363 (1992).

- <sup>26</sup>P. A. Sterne and J. H. Kaiser, Phys. Rev. B **43**, 13 892 (1991) used another type of parametrization for both the correlation potential (Ref. 8) and the enhancement factor (Ref. 9) but we do not use them here.
- <sup>27</sup>R. M. Nieminen and C. H. Hodges, Solid State Commun. **18**, 1115 (1976).
- <sup>28</sup>D. M. Schrader, Phys. Rev. A **20**, 918 (1979).
- <sup>29</sup>H. Stachowiak, Phys. Rev. B **41**, 12 522 (1990); H. Stachowiak and J. Lach, *ibid.* **48**, 9828 (1993).
- <sup>30</sup>G. Brauer, W. Anwand, E.-M. Nicht, P. G. Coleman, A. P. Knights, H. Schut, G. Kögel, and N. Wagner, J. Phys.: Condens. Matter **7**, 9091 (1995).
- <sup>31</sup>A. Rosencwaig, *Photoacoustic and Photoacoustic Spectroscopy* (Wiley, New York, 1980), pp. 125 and 177.
- <sup>32</sup>W. Schottky, Z. Phys. **113**, 367 (1939).
- <sup>33</sup>N. B. Chilton and P. G. Coleman, Meas. Sci. Technol. **6**, 53 (1995).
- <sup>34</sup>J. A. Powel and L. G. Matus, in *Springer Proceedings in Physics*, edited by G. L. Harris and C. Y.-W. Yang (Springer, Berlin, 1989), Vol. 34, p. 2.
- <sup>35</sup>G. Pensl and W. J. Choyke, Physica B **185**, 264 (1993).
- <sup>36</sup>G. Brauer, W. Anwand, P. G. Coleman, A. P. Knights, F. Plazaola, Y. Pacaud, W. Skorupa, J. Störmer, and P. Willutzki, Phys. Rev. B **54**, 3084 (1996).
- <sup>37</sup>L. Gilgien, Ph.D. thesis University of Geneva, 1997.
- <sup>38</sup>A. Harju, B. Barbiellini, S. Siljamäki, R. M. Nieminen, and G. Ortiz, Phys. Rev. Lett. **79**, 1173 (1997).
- <sup>39</sup>R. Suzuki, T. Ohdaira, A. Uedono, S. Ishibashi, A. Matsuda, S. Yoshida, Y. Ishida, S. Niki, P. J. Fons, T. Mikado, T. Yamazaki, S. Tanigawa, and Y. K. Cho, Mater. Sci. Forum **255-257**, 714 (1997).
- <sup>40</sup>J. P. Perdew and A. Zunger, Phys. Rev. B **23**, 5048 (1981).